Analytica Chimica Acta 826 (2014) 69–76

Contents lists available at ScienceDirect

Analytica Chimica Acta

journal homepage: www.elsevier.com/locate/aca

Development of a real-time capacitive biosensor for cyclic cyanotoxic peptides based on Adda-specific antibodies

Lesedi Lebogang [a], Martin Hedström [a,*], Bo Mattiasson [a,b]

[a] Department of Biotechnology, Lund University, Box 124, 22100 Lund, Sweden
[b] CapSenze HB, Annersbergs gård 5520, 26021 Billeberga, Sweden

HIGHLIGHTS

- Broad spectrum microcystin detection using Adda-specific monoclonal antibodies.
- Highly stable and sensitive bio-platform made from polytyramine and gold nanoparticles.
- Low detection limit of 2.1×10^{-14} M MC-LR standard and stability for 30 regeneration-assay cycles.
- Short analytical time and real-time information on antigen–antibody binding kinetics.
- Biosensor can be used for microcystin evaluation in environmental matrix with minimal sample preparation.

GRAPHICAL ABSTRACT

Specific monoclonal antibodies were immobilized on a gold surface modified with polytyramine and gold nanoparticles. Introduction of the target microcystin in the immunosensor resulted in a capacitance decrease whereas in the blank sample it remained unchanged.

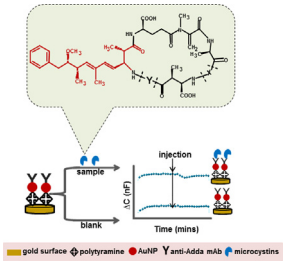

ARTICLE INFO

Article history:
Received 5 February 2014
Received in revised form 11 March 2014
Accepted 21 March 2014
Available online 26 March 2014

Keywords:
Cyclic cyanotoxins
Capacitive
Adda-specific antibodies
Electropolymerization
Gold nanoparticles

ABSTRACT

The harmful effects of cyanotoxins in surface waters have led to increasing demands for accurate early warning methods. This study proposes a capacitive immunosensor for broad-spectrum detection of the group of toxic cyclic peptides called microcystins (~80 congeners) at very low concentration levels. The novel analytical platform offers significant advances compared to the existing methods. Monoclonal antibodies (mAbs, clone AD4G2) that recognize a common element of microcystins were used to construct the biosensing layer. Initially, a stable insulating anchor layer for the mAbs was made by electropolymerization of tyramine onto a gold electrode surface, with subsequent incorporation of gold nanoparticles (AuNPs) on the glutaraldehyde (5%) activated polytyramine surface. The biosensor responded linearly to microcystin concentrations from 1×10^{-13} M to 1×10^{-10} M MC-LR standard with a limit of detection of 2.1×10^{-14} M. The stability of the biosensor was evaluated by repeated measurements of the antigen and by determining the capacitance change relative to the original response, which decreased below 90% after the 30th cycle.

1. Introduction

Drinking water authorities are concerned regarding the ever-increasing number of cyclic cyanotoxin variants produced during cyanobacterial blooming. Toxic cyanobacterial blooms are a global

* Corresponding author. Tel.: +46 46 222 7578; fax: +46 46 222 4713.
E-mail address: martin.hedstrom@biotek.lu.se (M. Hedström).

http://dx.doi.org/10.1016/j.aca.2014.03.028
0003-2670/

problem and their proliferation is partly intensified by eutrophication of water bodies from human activities [1–3] such as farming and cattle rearing. Cyanobacteria genera, such as *Microcystis*, *Nostoc*, *Anabaena* and *Oscillatoria* can produce substantial amounts of toxic peptides defined as microcystins, which are a group of cyclic hepatotoxic heptapeptides [4,5]. These toxic peptides are a human health threat since they are cancerogenous [6,7]. Moreover, recent studies have implicated them in decreased male reproductive capacity in mice [8]. Therefore, regular monitoring of these toxins should be prioritized considering that they are currently not efficiently removed by conventional water treatment processes [9,10].

Accurate determination of microcystins is primarily challenged by a large number of microcystin variants co-occurring in watercourses. To date, there are approximately 80 microcystin variants identified, which have varying hydrophobicities depending on the substituted amino acids in the structure [7,11,12], and this variety creates a considerable challenge for a single assay determination. The discovery/characterization of new and structurally different variants renders the existing detection methods inadequate since they are aimed at a single or few variants. Furthermore, concentrations of an individual toxin can be below the detection limits of many of the analytical methods currently employed [10,13,14]. Hence, a reliable and sensitive detection technique is required to measure the entire group of microcystins.

Recently, one area of development that has been extensively explored for trace analysis of microcystins is the biosensor approach. Biosensors based on various transduction principles, such as capacitive [15,16], surface Plasmon resonance [17], evanescent-wave excitement [4,18] have been reported. Although most of these biosensors are designed for one commonly studied microcystin variant; microcystin-leucine; arginine (MC-LR), recent advancements have reported biosensors that can detect the four variants with arginine in position 4 of their cyclic peptide structure (Fig. 1), by using monoclonal antibody (mAb, MC10E7) [17,19], which was produced and characterized by Zeck et al. [20]. Nevertheless, the analytical challenge remains as these biosensors are only selective to a limited number of variants and could miss detection of equally potent variants. Further improvements can be made by using other mAb-types, such as AD4G2 clone that is raised against a characteristic feature of all microcystins called 3-amino-9-methoxy-2,6,8-trimethyl-10-phenyldeca-4,6-dienoic acid (Adda) to detect all the existing microcystins [12,21,22].

Capacitive biosensors have become widely used to directly measure binding reactions of antibody–antigen on a gold surface [23,24] because of their ability to detect trace amounts of analytes as well as the user-friendliness of the method [25–27]. Exploiting the uniqueness of the Adda-moiety to microcystins, we used the AD4G2 mAbs as a sensing biomolecule to develop a broad-spectrum capacitive biosensor. In addition, the biosensor will also be able to detect the closely related Adda-containing cyclic pentapeptides (nodularins), which are produced by a salt tolerant cyanobacterium called *Nodularia spumigena* [6], as well as by a microcystin degradation products. As such, the sensor has the ability to tell the contamination history of the waters, making it well suited for use as an early warning tool for immediate intervention. In most parts of the world, surface water contributes immensely as the primary drinking water source, and occasionally experiences high eutrophication mainly from livestock and wild animals that drop their wastes during drinking [28]. Such sources are likely to experience cyanobacterial blooms that produce cyanotoxins, which will eventually affect drinking water purification. Hence, in this study cow urine in buffer was used to mimic real situation where the surface water could contain all kinds of compounds (both organic and inorganic).

2. Experimental

2.1. Materials and reagents

Microcystin standard (MC-LR) was purchased from Enzo Life Sciences, (Malmö, Sweden). Adda-specific monoclonal antibodies

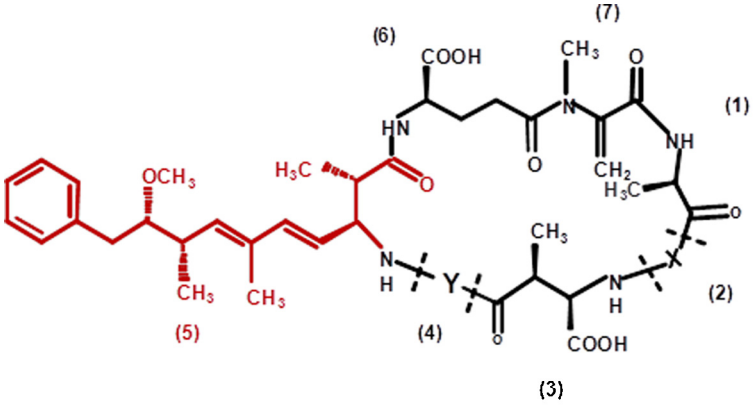

Microcystin variants	Position2 (X)	Position 4 (Y)
MCLR	leucine	arginine
MCLA	leucine	alanine
MCYR	tyrosine	arginine
MCRR	arginine	arginine
MCLW	leucine	tryptophan
MCLF	leucine	phenylalanine

Fig. 1. General cyclic structure of microcystins (D-Ala[1]-X[2]-D-MeAsp[3]-Y[4]-Adda[5]-D-Glu[6]-Mdha[7]). Adda moiety-a characteristic microcystin amino acid, X and Y represent variable L-amino acids at positions 2 and 4 respectively, and examples of some of the commonly reported microcystin variants that co-occur in waters.

(AD4G2) were purchased from Abraxis LLC (Warminster, PA, USA). Tyramine, HPLC grade methanol and 1-dodecanethiol were from Sigma–Aldrich (Steinheim, Germany). Ethanol, sodium hydroxide and all other chemicals used for buffer preparation were of analytical grades and were used as received. Ultrapure water was obtained from the Milli-Q (18.2 ΩM cm) purification system (Millipore, Bedford, MA, USA). Alumina slurry (0.3 and 0.1 μm) was from Struers (Ballerup, Denmark). AuNPs were made in-house according to the work of Loyprasert et al. [29] in our group.

2.2. Preparation of the biorecognition layer

Fabrication of the biorecognition layer is exceedingly important since it is the basis of the biosensor's sensitivity and stability, and hence reproducibility of the results. As such, the biomolecule has to be treated in such a way that its biological activity is not compromised. In order to achieve this, gold electrodes (diameter 3 mm) were cleaned using alumina slurry following the procedure in Hedström et al. [26]. A thin layer of polytyramine was electrodeposited on the cleaned gold surface to function as surface insulation and anchor for antibodies. Electropolymerization was performed in a freshly prepared tyramine (100 mM) dissolved in methanol containing 300 mM NaOH solution. Fifteen cycles were run in a 3-electrode electrochemical cell using Autolab potentiostat (8 PGSTAT12, Eco Chemie, The Netherlands) to perform cyclic voltammetric scanning between 0 V and 1.5 V (vs Ag/AgCl) at a scan rate of 50 mV s^{-1} [27]. The electrode surface was then washed with pure water to remove unpolymerized tyramine. Glutaraldehyde (5%) in potassium phosphate buffer (10 mM, pH 7.2) was used to activate the polytyramine layer for 20 min and the electrodes were again washed with the buffer. This was followed by drop-coating the electrodes with 10 μL of colloidal solution of AuNPs, and incubating for 6, 12 and 24 h (4 °C) to allow the citrate stabilized AuNPs to adsorb via the resultant aldehyde group [30] and possible unreacted amino groups of tyramine.

After incubation, non-adsorbed AuNPs were washed off with pure water followed by phosphate buffer, and dried with a stream of nitrogen gas. The electrodes were then ready for antibody immobilization. Ten microliters of 25 mg L^{-1} anti-Adda mAbs were deposited on the electrodes and left to adsorb overnight. The interactions on the electrode surface are electrostatic between the negatively charged AuNPs and the positively charged amino groups of antibodies. As the next step, to block any bare spaces on the electrode surface, electrodes were treated with 10 mM 1-dodecanethiol in ethanol prior to use in a flow cell. Finally, the electrodes were further treated with ethanolamine (100 mM, pH 8) to block any possible non-reacted aldehyde groups that resulted from activation with glutaraldehyde. All buffer solutions used were prepared using pure water obtained from the Milli-Q system (18 ΩM cm) and filtered through 0.22 μm filters and degassed.

2.3. Capacitance measurements

In an automated 3-electrode flow-cell capacitance system (CapSenze Biosystems, CapSenze HB, Lund, Sweden), the previously modified gold electrode was used as a working electrode while two platinum wires were used as reference and auxiliary electrodes. The system presents a fully automated sample analysis with software-controlled capacitance measurements (Fig. 2). The in-house developed capacitive system uses current charge and measures the resulting potential according to Eq. (1) [31] as opposed to the potential perturbation system used before, where a certain potential was applied to the electrode and the responding current was measured.

$$C = \frac{I \times t}{U} \tag{1}$$

where C is the total capacitance, I is the current supplied to the sensor, t is the current pulse period and U is the slope of the voltage built up across the surface. The signal is automatically calculated and displayed on the monitor as capacitance change (ΔC, Farad).

Capacitance measurements apply the electrical double layer theory, that when capacitors are arranged in series, the total capacitance measured at an electrode–electrolyte interface is expressed as Eq. (2).

$$\frac{1}{C_{tot}} = \frac{1}{C_{ins}} + \frac{1}{C_{bio}} + \frac{1}{C_{dl}} \tag{2}$$

where C_{tot} is the total capacitance, C_{ins}, C_{bio} and C_{dl} are capacitance contributions from insulating, biosensing and diffuse layers respectively. According to Eq. (2), the lowest capacitance will dominate the total capacitance, therefore capacitance of the contributing layers should be as large as possible for the binding of analyte to elicit significantly dominating capacitance change (ΔC) [23]. ΔC (nF cm^{-2}) for a given binding event is expressed as the difference between C_{tot} (nF) before and after analyte binding divided by the active surface area (0.071 cm^2) of the electrode.

2.4. Assay performance

The assay was conducted according to Teeparuksapun et al. [27] with some modifications. Briefly, after inserting the working electrode into the flow-cell, a stream of 10 mM phosphate buffer (pH 7.2) used as running buffer, was pumped through the system at

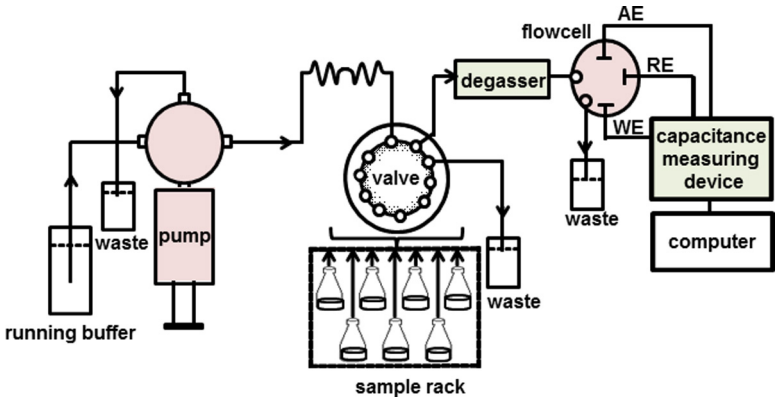

Fig. 2. An automated capacitive system used for the detection of microcystins. All these components are integrated into a box to make a single unit that is portable.

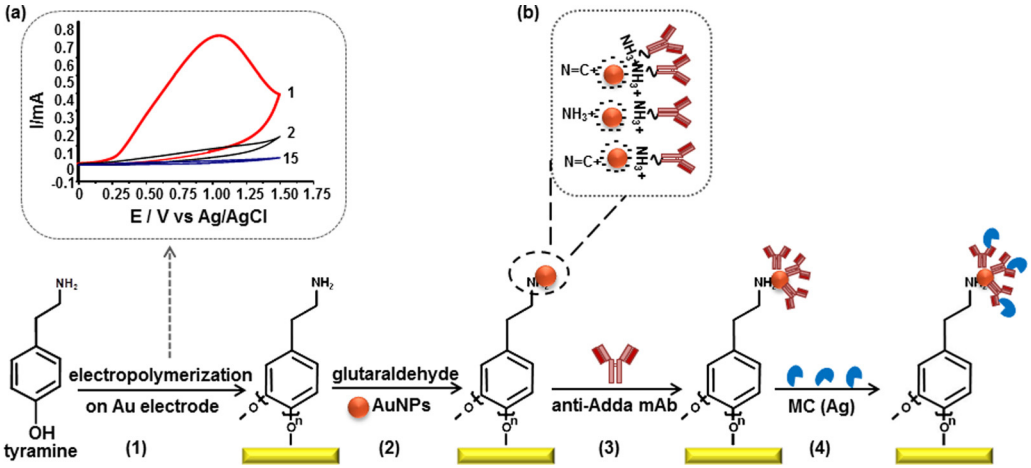

Fig. 3. Stepwise modification of gold electrode by electropolymerization of tyramine and immobilization of antibodies and subsequent antigen binding. Insets (a): cyclic voltammograms showing the oxidation peak behavior during electropolymerization of 10 mM tyramine dissolved in methanol containing 300 mM NaOH on a gold electrode, (b): reactions involved during glutaraldehyde and AuNPs treatment.

a flow rate of 100 μL min^{-1} to allow stabilization of the sensing layer. After achieving a stable baseline, 250 μL of the diluted standard samples were automatically injected into the flow-cell and the capacitance change was monitored. The biosensing layer was prepared for the next assay by breaking Ab–Ag interaction using 25 mM glycine–HCl buffer (pH 2.5).

Microcystin standard stock solution was prepared by reconstituting the lyophilized microcystin powder in 100% methanol and was stored at −20 °C until use. Different standard concentrations were prepared by serial dilutions of the stock solution using running buffer, resulting in a negligible concentration of methanol in the samples. The sample vials were then inserted into respective injection loops according to the set program, where sample rack can handle seven vials at a time including a regeneration solution vial (Fig. 2).

2.5. Optimization and stability

Optimization of the system was done mainly on 10 mM potassium phosphate buffer (pH 7.2) and 15 mM Tris–HCl (pH 7.2) buffers. Different times of AuNPs immobilization (6, 12, and 24 h) were also investigated. Stability tests were carried out by repeated measurements of 1.0×10^{-12} M standard solution diluted in phosphate buffer (10 mM, pH 7.2) with 6 h immobilization period of AuNPs. Our study was limited to MC-LR during development and optimization of the biosensor. The use of one microcystin variant, in particular MC-LR, was considered sufficient because of the similar cross-reactivities between the variants [32]. MC-LR is generally used as a representative microcystin because it is widely studied and commercially available at relatively low costs.

2.6. Matrix effects

Minimal sample preparation is a general goal in the field of bioanalysis as it reduces analytical costs and avoids sample loss from the many steps of pre-treatment. The presence of other compounds/components in the sample matrix often impedes accurate and specific measurement of the target [24,33]. Since the sensor is intended for use around many ponds of fresh water where cattle may be grazing, and there is risk of urine contamination although in very dilute form. Urine is a complex medium that comprises urinary proteins (albumin and amino acids) and urea [34] as well as inorganic ions such as potassium, sodium and ammonium. Therefore, robustness of the biosensor to withstand interferences from components that may be present in the sample during analysis was investigated using cow urine. Fresh cow urine was collected and frozen at −20 °C until analysis. Different dilutions of the raw urine samples were tested on the modified biosensor electrode to determine the influence of a complex matrix on the capacitance measurements. The urine samples were spiked with known microcystin concentrations and appropriate dilutions were made with phosphate buffer solution to reach the desired final concentrations for use in the biosensor analysis. Percentage recoveries were calculated from the obtained capacitive measurement results according to Eq. (3).

$$\%\,\text{Recovery} = \frac{\text{spiked} - \text{unspiked}\,(\textit{blank})}{\text{known spike added}} \quad (3)$$

3. Results and discussion

3.1. Grafting of the biosensing layer

The sensitivity of the capacitive biosensing layer is highly dependent on a well-built, stable and isolating transducer (i.e., working electrode modifications and antibody immobilization approach). Hence, the gold electrode surface was modified with AuNPs attached to a glutaraldehyde activated polytyramine layer to form a suitable platform for antibody immobilization. AuNPs provide an increased surface area of the biosensing layer for dense immobilization of antibody, thereby amplifying the signal [27,35]. The stability arises from the electrostatic binding forces that are created between the negatively charged AuNPs and positively charged Schiff base [36] and possible non-activated amino groups from the polytyramine layer as illustrated in Fig. 3, inset (b). The stability resulting from the combination of resultant aldehyde group and AuNPs has been previously described [36] but for a different purpose than biosensing. Zhang and Wu [36] further observed that AuNPs treated with $NaBH_4$ form a stable assembly that further improves the layer stability during the modification process.

Electrodeposition of tyramine creates a thin uniform layer that improves sensitivity [37] as shown in Fig. 3, inset (a), cyclic voltammograms depicting an irreversible oxidation of tyramine. The first scan shows a strong oxidation/redox peak around 1 V, which dramatically decreases and ultimately disappears on subsequent cycles. The diminishing oxidation peak indicates the

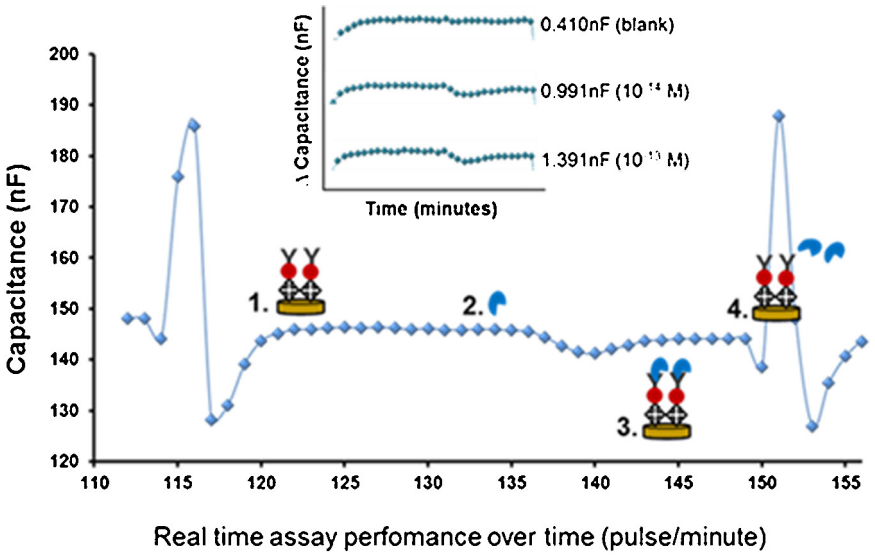

Fig. 4. Actual capacitive sensorgrams showing real-time binding signal (1.0×10^{-14} M) with a total assay time of 37 min (22 min regeneration and baseline stabilization and 15 min sample binding reaction). Numbered phases represent: (1) stable baseline; (2) injection; (3) binding and (4) regeneration and each point represents a pulse. Inset: sensor response to the different concentrations of MC-LR.

deposition of the non-conducting polytyramine on the transducer surface [37,38]. The polytyramine layer is self-limiting in growth, which results in thin films that bring functionalized sites closer to the electrode surface, giving sensitive detection and pronounced capacitance signals [23].

The concentration of the Adda-specific antibodies used (25 mg L^{-1}) was appropriate for this study, which is demonstrated by a pronounced capacitance reduction signal in Fig. 4. After extensive literature search about similar cross-reactivities of microcystins and nodularins, the indication is that the Adda moiety displays a relative immunodominance to Adda-specific antibodies and hence will recognize all microcystins present in a sample. The meticulous work of commercially available Adda-specific mAbs (AD4G2) has reported high cross-reactivities (Table 1) to all microcystins that were tested [22,32]. Fischer et al., [12] also produced mAbs against this unusual amino acid (Adda) and developed a method for the direct competitive ELISA based on this antibody. They created a cross-reactivity pattern that showed highly similar response for different microcystins. The ELISA kit has been approved and is commercially available as the total microcystin determination kit.

Moreover, similar responses have been obtained for several different MCs on the immunosensors [39–41] and some are shown in Table 1, deducing the conclusion that microcystin antibodies give high cross-reactivity toward microcystins due to their similar common structural moiety. Therefore, the selectivity of Adda-specific antibodies to the entire microcystin group cannot be argued since they recognize the conserved moiety, which is also thought to be significant for toxicity of microcystins. Furthermore, with the manufacturer's recommendation that only one calibration curve (preferably MC-LR) should be made because the cross-reactivity between variants is very high [32], our study was limited to one variant (MC-LR).

Based on the above analysis, it is believed that the selective distinction for microcystins is hardly realized due to their highly similar cyclic structure with the Adda moiety hanging on the side. Alternatively, cumulative determination of a mixture of microcystin variants was assessed in a further study not part of this work. The results were compared to the ones obtained from a commercial ELISA kit using the same antibodies. The two methods correlated well with a regression line of $y = 0.873x + 0.164$ and coefficient of 0.992 [42]. The use of Adda antibodies definitely simplifies the assay work by eliminating the need to use several standards, some which are not commercially available or unknown.

3.2. Optimization of assay parameters

Potassium phosphate and Tris–HCl buffers were evaluated and since the former performed better it was used for the rest of the experimental work. The AuNP immobilization intervals investigated (6, 12 and 24 h) significantly influenced the stability and degree of insulation of the biosensing layer and hence the electrode performance. The 6 h interval was chosen due to the stable baseline level acquired. The 12 and 24 h immobilization intervals resulted in similar baseline stabilities but with significantly lower recorded sensitivity (*data not shown*), implying a situation of a too insulated surface. Furthermore, the surfaces where gold nanoparticles were immobilized for 12 and 24 h seemed to be easily eroded during assaying. The observed differences could be interpreted as that during extended time of immobilization, AuNPs built up forming multilayers instead of monolayers. Although capacitance measurements are strongly dependent on electrical insulation of the biosensing layer, too much insulation affects its sensitivity. As explained earlier, it

Table 1
Cross-reactivities obtained with antibodies directed to a group of microcystins.

Method	Antibody	Variants	Cross-reactivity	References
ELISA	MC-159 mAb	MC-LR, -YR and -LA, nodularins	>88%	[40]
Optical microsensor arrays	MC mAb	MC-LR, -LA, -LF, -LW, -LY, -YR and nodularins	83–144%	[14]
ELISA	AD4G2 mAb	All 14 microcystins tested	51–163%	[22]
ELISA	Adda-specific	MC-LR, -RR, -YR, -LW, -LF, demethylated MC-LR and -RR	50–167%	[12]

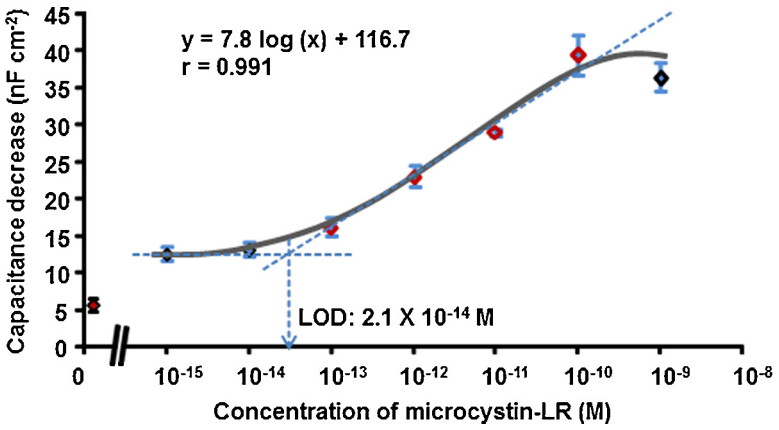

Fig. 5. Capacitance decrease against log concentration of MC-LR in phosphate buffer (10 mM, pH 7.2). The point (◆) shows the background noise of the blank (buffer).

creates a thick layer between the electrode surface and the recognition sites [23].

3.3. Biosensor performance

With a stable biosensing layer, the antibody–antigen binding interactions were followed as the capacitive assay proceeded and the data stream was observed in real-time (Fig. 4). The overall assay time, including the regeneration cycle (using glycine–HCl) was determined to 37 min, which could be considered as rather rapid in comparison to conventional methods for microcystin detection. The short assay time also indicates that the capacitive technology could be suitable for on-site analysis.

The introduction of the target microcystin in the biosensor system resulted in a capacitance decrease, which varied according to different concentrations applied (Fig. 4, inset). Owing to the specific interaction of the microcystin and the immobilized Adda-specific antibodies, the microcystin standard concentrations induced a significant capacitance change whereas the change was negligible for the blank. The biosensor responded linearly to microcystin concentration between 1.0×10^{-13} M and 1.0×10^{-10} M, and a limit of detection (LOD) of 2.1×10^{-14} M MC-LR, which was calculated according to IUPAC guidelines [43]. The LOD achieved in this work is several orders of magnitude below the World Health Organization (WHO) guideline of 1 μg L^{-1} (1.0×10^{-9} M) for drinking water [44]. A comparable LOD has been achieved in another capacitive detection of microcystins [45]. Moreover, this capacitive method has been applied in determination of other different biomolecules and achieved subattomolar LODs [26,28]. The calibration equation is ΔC (nF cm^{-2}) = 7.8 log (x) + 116.7 with a correlation coefficient of 0.991 (n = 4) (Fig. 5). The high sensitivity offers an advantage of reducing environmental matrix effects by diluting samples without losing the detectable levels of the analyte during the analysis of real samples [24].

3.4. Stability of the biosensor

The number of times an assay platform could be reused is of particular importance in routine monitoring purposes where frequent use may prove to be costly. The stability and reusability of the biosensing layer were therefore evaluated by repeated measurements of capacitance using the 1.0×10^{-12} M standard, and reproducibility was determined by the amount of capacitance change relative to the original response (100%). As depicted in Fig. 6, the biosensor maintained a stable binding capacity of 95 ± 3.7% for 30 regeneration-assay cycles before showing any significant performance reduction (below 90%), and the modified electrode remained fully-active up to 7 days of moist storage at 4 °C. Since the storage stability of the electrode has remained a challenge for biosensors in general, mainly due to the instability of the immobilized biomolecules, the reduction in binding capacity of the biosensor could be ascribed to that the antibodies gradually lost their activity [27]. The fact that the experiments were performed at room temperature for extended periods could imply that the integrity of the immobilized antibodies deteriorated with time. The destruction of the biosensing platform is unlikely to be the reason for performance reduction because the baseline tends to return to the previously established level, affirming that the insulating properties were intact.

3.5. Matrix effects on analytical performance

Matrix effects can adversely affect the biosensor performance by either suppression or enhancement of biorecognition layer'-sensitivity as well as introducing highly interfering contaminants, thus giving unwanted non-specific binding [24] as well as conductive influences. From the above notion, the biosensor was evaluated for possible interferences from the environmental matrix by using non-spiked urine samples. In Fig. 7 capacitance results showed that the biosensor was affected by the presence of high urine concentrations. The interferences were mainly conductivity related. Since salt ions demonstrated to have a significant influence on capacitance measurements on previous studies [23,33], the results are reasonable because urine contains some salt ions such as potassium, sodium and others, therefore the sensor is limited to low ionic strength media.

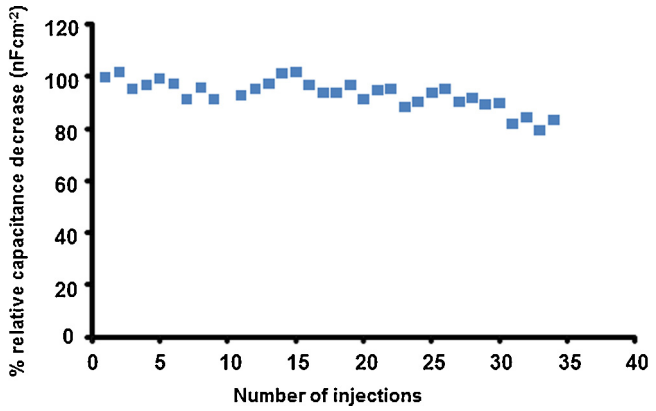

Fig. 6. Reusability of the electrode using 1.0×10^{-12} M standard with injection volume of 250 μL.

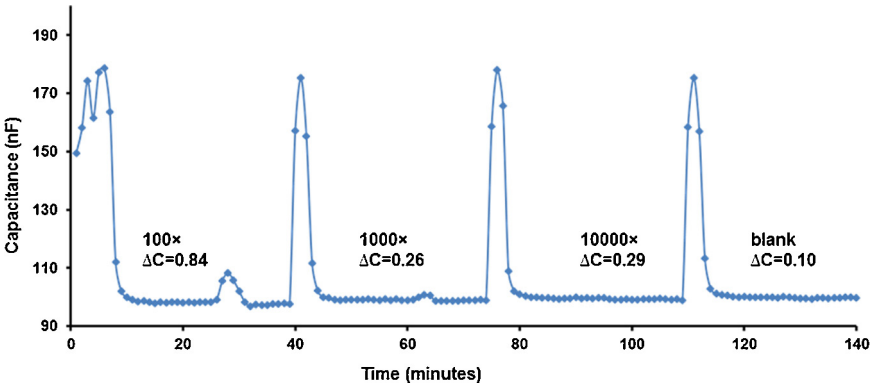

Fig. 7. Actual capacitive responses from different non-spiked urine dilutions during matrix effect investigations.

Table 2
Recoveries of microcystins spiked in different urine dilutions obtained using the developed capacitive biosensor.

Sample dilutions	Spiked concentration (M)	Calculated concentrations ($\times 10^{-12}$ M)	% Recovery	% CV
Buffer	1.00×10^{-12}	1.06 ± 0.11	106 ± 11	10.0
Urine (1000×)	1.00×10^{-12}	1.11 ± 0.13	111 ± 13	11.9
Urine (10,000×)	1.00×10^{-12}	1.03 ± 0.10	103 ± 10	9.50

A 100× dilution was considered not suitable for evaluation since it showed a higher background signal (Fig. 7) compared to subsequent dilutions of the non-spiked urine samples. Moreover, it highly affected the dielectric properties of the biosensor, indicating that high salt concentrations are still present. Upon optimization of the urine dilutions (1000× and 10,000×) with the carrier buffer, the biosensor response was relatively comparable between the buffer and spiked urine samples as summarized in Table 2. The percentage recoveries were 106, 111 and 103 for spiked samples diluted in buffer, 1000 and 10,000× urine respectively.

The conductive influence suggests that urine might be a too complex matrix to operate the sensor and minor sample pretreatments are still needed unless in very dilute situations, but considering that urine will always be diluted in environmental waters could render the biosensor applicable.

4. Conclusions

A rapid capacitance-based biosensor was developed using Adda-specific mAbs that recognize the conserved element of the group of microcystins. The easy-to-use capacitive biosensor unit demonstrated direct antibody–antigen interaction in real-time. The antibody immobilization strategy formed a stable biosensing layer that allowed sensor reusability of up to 30 times before showing significant deterioration. Signal amplification was achieved using AuNPs to increase the surface area for dense antibody attachment on the biosensing layer. Furthermore, the biosensor sensitivity (LOD = 2.1×10^{-14} M MC-LR) satisfies the WHO requirement and therefore stands as an ideal tool for multiple toxin detection. Performance interference from environmental pollutants is a factor that could render biosensor application to real samples more complicated but with proper dilutions accurate sensitivity could be achieved. Some factors such as matrix interference and storage stability still need improvements, particularly by developing immobilization strategies that offer more stable functionalities.

Acknowledgement

This work was supported by the Government of the Republic of Botswana, under the auspices of Botswana International University of Science and Technology PhD. studies.

References

[1] G.A. Codd, Ecological Engineering 16 (2000) 51–60.
[2] L. Spoof, P. Vesterkvist, T. Lindholm, J. Meriluoto, Journal of Chromatography A 1020 (2003) 105–119.
[3] S. Bogialli, M. Bruno, R. Curini, A. Di Corcia, A. Lagana, B. Mari, Journal of Agricultural and Food Chemistry 53 (2005) 6586–6592.
[4] F. Long, M. He, A.N. Zhu, H.C. Shi, Biosensors and Bioelectronics 24 (2009) 2346–2351.
[5] W.W. Carmichael, Journal of Applied Bacteriology 72 (1992) 445–459.
[6] K. Sivonen, G. Jones, in: I. Chorus, J. Bertram (Eds.), Toxic Cyanobacteria in Water: A Guide to Their Public Health Consequences, Monitoring and Management, E and FN Spon, London, 1991, pp. 41–111.
[7] D.R. Dietrich, S.J. Hoeger, Toxicology and Applied Pharmacology 203 (2005) 273–289.
[8] Y. Chen, J. Xu, L. Yan, X. Han, Reproductive Toxicology 31 (2011) 551–557.
[9] M.G. Antoniou, A.A. de la Cruz, D.D. Dionysiou, Journal of Environment Engineering 13 (2005) 1239–1243.
[10] D.R. Dietrich, A. Fischer, C. Michel, S.J. Hoeger, in: K.H. Hudnell (Ed.), Cyanobacterial Harmful Algal Blooms: State of the Science and Research Needs, 619, Advances in Experimental Medicine Biology, 2008, pp. 885–912.
[11] I.S. Kim, G.H. Nguyen, S. Kim, J. Lee, H. Yu, Environmental Engineering Research 14 (2009) 250–254.
[12] J.W. Fischer, I. Garthwaite, C.O. Miles, K.M. Ross, J.B. Aggen, A.R. Chamberlin, N. R. Towers, D.R. Dietrich, Environmental Science & Technology 35 (2001) 4849–4856.
[13] K. Lahti, J. Rapala, A.-L. Kivimäki, J. Kukkonen, M. Niemelä, K. Sivonen, Water Science and Technology 43 (2001) 225–228.
[14] S. Morais, J. Tamarit-Lopez, R. Puchades, A. Maquieira, Environmental Science & Technology 44 (2010) 9024–9029.
[15] X. Sun, H. Shi, H. Wang, L. Xiao, L. Li, Analytical Letters 43 (2011) 533–544.
[16] S. Loypraset, P. Thavarungkul, P. Asawatreratanakul, B. Wongkittisuksa, C. Limsakul, P. Kanatharana, Biosensors and Bioelectronics 24 (2008) 78–86.
[17] T. Vinogradova, M. Danaher, A. Baxter, M. Moloney, D. Victory, S.A. Haughey, Talanta 84 (2011) 638–643.
[18] M. Campás, J.-L. Marty, Biosensors and Bioelectronics 22 (2007) 1034–1040.
[19] S. Herranz, M.D. Marazuela, M.C. Moreno-Bondi, Biosensors and Bioelectronics 33 (2012) 50–55.

[20] A. Zeck, A. Eikenberg, M.G. Weller, R. Niesser, Analytica Chimica Acta 441 (2001) 1–13.
[21] B.C. Hitzfeld, S.J. Höeger, D.R. Dietrich, Environmental Health Perspectives 108 (2000) 113–122.
[22] A. Zeck, M.G. Weller, D. Bursill, R. Niessner, Analyst 126 (2001) 2002–2007.
[23] C. Berggren, B. Bjarnason, G. Johansson, Biosensors and Bioelectronics 13 (1998) 1061–1068.
[24] B. Mattiasson, K. Teeparuksapun, M. Hedström, Trends in Biotechnology 28 (2009) 20–27.
[25] I. Bontidean, C. Berggren, G. Johansson, E. Csöregi, B. Mattiasson, J.R. Lloyd, K.J. Jakeman, N.L. Brown, Analytical Chemistry 70 (1998) 4162–4169.
[26] M. Hedström, I.Y. Galaev, B. Mattiasson, Biosensors and Bioelectronics 21 (2005) 41–48.
[27] K. Teeparuksapun, M. Hedström, E.Y. Wong, S. Tang, I.K. Hewlett, B. Mattiasson, Analytical Chemistry 82 (2010) 8406–8411.
[28] B.A. Siame, D.D. Shushu, H.M. Masundire, Mycotoxins and Phycotoxins in Perspective at the Turn of the Millenium, in: W.J. de Koe, R.A. Samson, H.P. van Egmond, J. Gilbert, M. Sabino (Eds.), Ponsen & Looyen, Wageningen, The Netherlands, 2001, pp. 445–451.
[29] S. Loyprasert, M. Hedström, P. Thavarungkul, P. Kanatharana, B. Mattiasson, Biosensors and Bioelectronics 25 (2010) 1977–1983.
[30] K. Teeparuksapun, P. Kanatharana, W. Limbut, C. Thammakhet, P. Asawatreratanakul, B. Mattiasson, B. Wongkittisuksa, C. Limsakul, P. Thavarungkul, Electroanalysis 21 (2009) 1066–1074.
[31] D. Erlandsson, K. Teeparuksapun, B. Mattiasson, M. Hedström, Sensors and Actuators B 190 (2014) 295–304.
[32] Microcystins and other cyanobacterial toxins. Enzo Life Sciences, product flyer. International Edition, February 2010.
[33] K. Zor, R. Ortiz, E. Saatci, R. Bardsley, T. Parr, E. Csöregi, M. Nistor, Bioelectrochemistry 76 (2009) 93–99.
[34] K. Nakamoto, R. Kurita, O. Niwa, Biosensors and Bioelectronics 26 (2010) 1536–1542.
[35] J.M. Pingarrón, P. Yáñez-sedeño, A. González-Cortés, Electrochimica Acta 53 (2008) 5848–5866.
[36] Z. Zhang, Y. Wu, Langmuir 27 (2011) 9834–9842.
[37] Z. Wu, J. Li, T. Deng, M. Luo, G. Shen, R. Yu, Analytical Biochemistry 337 (2005) 308–315.
[38] D. Losic, C. Martin, H. Thissen, N.H. Voelcker, Surface Science 584 (2005) 245–257.
[39] J. Sheng, M. He, H. Shi, Analytica Chimica Acta 603 (2007) 111–118.
[40] N. Khreich, P. Lamourette, P. Renard, G. Clavé, F. Fenaille, C. Créminon, H. Volland, Toxicon 53 (2009) 551–559.
[41] M. Lotierzo, R. Abuknesha, F. Davis, I.E. Tothill, Environmental Science & Technology 46 (2012) 5504–5510.
[42] L. Lebogang, B. Mattiassson, M. Hedström, Microchimica Acta (2014), doi:10.1007/s00604-014-1199-4.
[43] R.P. Buck, E. Lindner, Pure and Applied Chemistry 66 (1994) 2527–2536.
[44] WHO, Guidelines for Drinking-Water Quality, 2nd Ed., World Health Organisation, Geneva, 1998 Addendum to Vol.1.
[45] S. Dawan, P. Kanatharana, B. Wongkittisuksa, W. Limbut, A. Numnuam, C. Limsakul, P. Thavarungkul, Analytica Chimica Acta 699 (2011) 232–241.